Proc. of the 6th Intl. Symposium on Reliability Engineering and Risk Management (6ISRERM)
31 May – 1 June 2018, Singapore
Editor(s) Xudong Qian, Sze Dai Pang, Ghim Ping Raymond Ong, Kok-Kwang Phoon

EFFECTS OF SEISMIC SEQUENCE ON SDOF STRUCTURE WITH PINCHING HYSTERETIC BEHAVIOR

WUCHUAN PU and MING WU

Department of Civil Engineering, Wuhan University of Technology, Wuhan, China.
E-mail: puwuchuan@whut.edu.cn

Abstract

Building structures composed by timber materials are characterized by the slip type hysteresis that indicates degraded stiffness and strength. Due to the considerable loading history effect of this kind of structures, they may become more prone to failure when subjected to sequential seismic excitations. This paper investigates the effect of the seismic ground motion sequences on the ductility demand and residual displacement of building structures represented by slip-type hysteretic models. The single-degree-of-freedom (SDOF) structure is considered, which is modeled by the hysteretic model consisting of a slip element and a bilinear element. The seismic ground motion sequences are simulated by repeating the ground motions with different scale factors. Through dynamic time history analysis, the effect of seismic intensity, ductility level, hysteretic parameters, and site conditions are investigated. It was found that the seismic sequence has considerable effect on the ductility demand of short period structures located in hard soil sites. The residual displacement was presented by the ratio of residual displacement to the maximum displacement, and this ratio approximately obeys an exponential probability distribution. Based on the numerical results, the empirical formulas for estimating the ductility demand and the probability density distribution of residual displacement were established.

Keywords: Seismic sequence, aftershock, pinching hysteretic structure, residual displacement.

1 Introduction

In earthquake hazard-prone regions, building structures are potentially subjected to seismic sequence events characterized by an earthquake followed by aftershocks with comparable or even higher magnitude (Di Sarno 2013). Aftershock ground motions can cause substantial harm to the damaged structures subjected to a mainshock (Kam 2011). In current seismic code, however, design earthquake is defined as single event and the effects of seismic sequences have not been taken into account. Recently, some studies have tried to explore the influence of the seismic sequences on seismic response of structures with different hysteretic behaviour. It has been revealed that the seismic sequences produce responses that different from those obtained from single event, and the effect depends on a lot of factors including structural period, structural modeling approach, hysteretic model, damping ratio, frequency contents of ground motions, among others. The hysteretic models used in previous studies include bilinear model (Hatzigeorgiou and Beskos 2009) and modified Clough model (Amadio et al. 2003), which are usually employed to simulate steel structure or concrete structure, respectively. Those models did not include the pinching effect of hysteresis, which is instead a typical phenomenon for timber structures. Experimental studies have shown that timber-framed buildings have a very

limited energy dissipation capability due to the pinching phenomenon in its hysteretic loop, and the slip phenomenon is accompanied with degradation of strength and stiffness. These characteristics are significantly differentiated from those of other major construction materials, e.g. steel or concrete.

Compared to other types of materials, timber structures are expected to experience more significant degradation of structural performance due to the same level of ductility, so the structure damaged in a seismic even is considered more prone to a sequential event. In order to clarify the effects of seismic sequence on structural performance of pinching hysteretic structures, this study carries out numerical studies on this type of structures. Through a large number inelastic time history analysis, the ductility and residual displacement caused by ground motion sequences are investigated.

2 Hysteretic Models of Structures

Figure 1 shows the pinching hysteretic model (right-side), which is idealized from typical hysteresis of timber structures from experiments. The model has tri-linear skeleton curve, of which the first, second and third stiffness are denoted by K_1, K_2 and K_3, respectively. This model can be simulated by a combination of a bilinear model (left-side) and a slip model (middle). The initial elastic stiffness and post-yield stiffness of bilinear element are denoted by K_{B1} and K_{B2}, respectively, and those of slip element are denoted by K_{S1} and K_{S2}, respectively. The energy dissipation is contributed by the bilinear model in stationary vibration state. Figure 2 displays four different pinching hysteretic models with different parameters, which will be used in the following studies. They are differentiated by two parameters, namely H ($=K_{B2}/K_{B1}$) and P ($=K_{B1}/K_1$). Within the four models, the one with P=0.53 and H=0.0566 is obtained from experiment on typical brace-type timber frames (Matsuda and Kasai 2015), and the other three models are assumed for parametric studies. The period of SDOF structure is set to be 0.5 s, 0.8 s, 1.2 s and 2.0 s, respectively. The constant value of u_c=0.45 cm and u_y=1.8 cm are defined for all models.

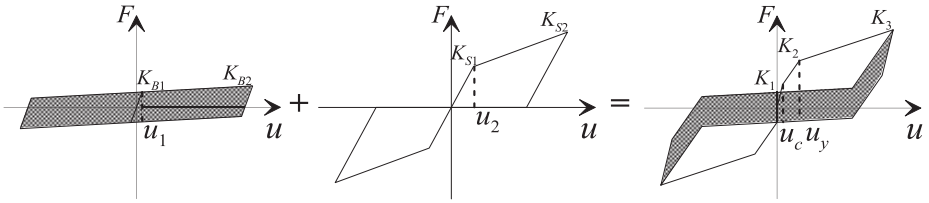

Figure 1. Pinching hysteretic model

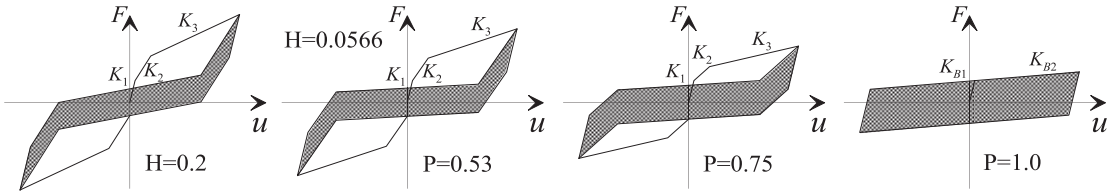

Figure 2. Different hysteretic models considered in this study

3 Model of Seismic Sequence

A variety of methods have been used to simulate the seismic sequences, including replicating the same ground motion, real recorded sequential ground motions, random combinations of different ground motions (Hatzigeorgiou 2010), and spectra matched ground motions (Shin and Kim

2017). On the other hand, it was reported that aftershock is very different with the mainshock in their frequency components and spectral characteristics etc. In this study, the seismic sequences are simulated by scaling the ground motion recorded in earthquake events. A total of 40 ground motions were selected from the strong motion database of the Pacific Earthquake Engineering Research (PEER) Center. These ground motions were recorded in 4 different site categories (based on the definitions of the USGS). The peak ground acceleration of all ground motions are greater than 0.1 g. Each sequence consists of two ground motions, of which the PGA (peak ground acceleration) are scaled to 0.1 g, 0.2 g, 0.3 g, 0.4 g, 0.5 g and 0.6 g, respectively, and for each ground motion, 36 (6×6) sequences are obtained. Figure 3 shows the spectra of all selected ground motions and the spectral average of each soil type. Figure 4 shows two examples of seismic sequence combinations.

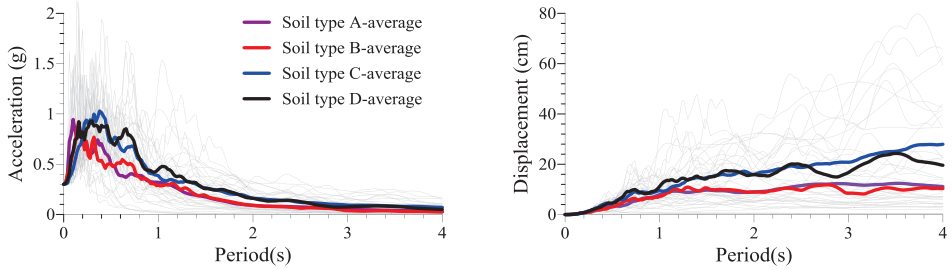

Figure 3. Acceleration and displacement response spectra of selected ground motions

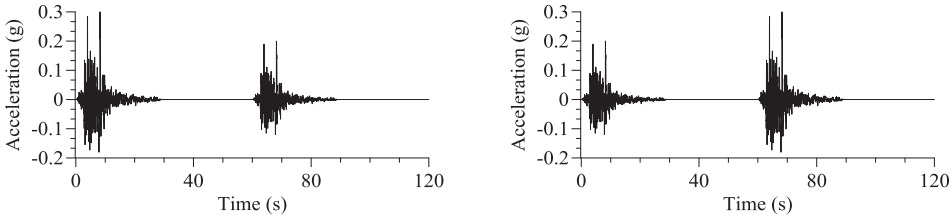

Figure 4. Two examples of seismic sequences

4 Numerical Results and Discussion

Time history analysis is performed on SDOF structures with assumed parameters. For each structural model, a total of 1440 (40 ground motions × 36 seismic sequences) cases of analyses are examined. The maximum displacements of structure caused by the two sequential ground motions are denoted by M_1 and M_2, and the corresponding residual displacement are denoted by R_1 and R_2, respectively.

4.1 *Maximum Displacement*

4.1.1 *Ductility Demand Amplification due to Seismic Sequence*

The structure damaged by the first ground motion is expected to experience more serious damage from the second ground motion. In order to present this effect quantitatively, the displacement ratio M_2/M_1 is plotted versus the intensity ratio PGA_2/PGA_1. All the time history analysis results with $M_1<u_c$ are excluded, therefore M_2/M_1 also denotes the ductility demand ratio. Figure 5 shows the relation between M_2/M_1 and PGA_2/PGA_1 for structural models with H=0.0566 subjected to ground motions recorded in soil type A. In a logarithmic coordinate, M_2/M_1 is approximately proportional to PGA_2/PGA_1. The relation between M_2/M_1 and PGA_2/PGA_1 is fitted by an exponential function as Eq.(1).

$$M_2/M_1 = \alpha(PGA_2/PGA_1)^{\beta} \tag{1}$$

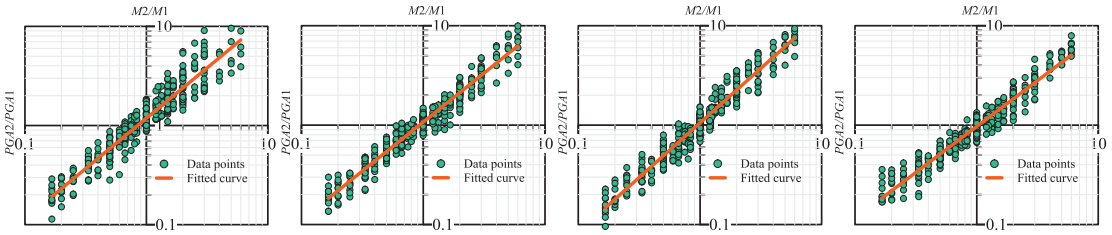

(a) *Class A, H*=0.0566, *T*=0.5*s* (b) *Class A, H*=0.0566, *T*=0.8*s* (c) *Class A, H*=0.0566, *T*=1.2*s* (d) *Class A, H*=0.0566, *T*=2.0*s*

Figure 5. The relation between M_2/M_1 and PGA_2/PGA_1

Table 1. The values of α and β identified from numerical results (*H*=0.0566 and 0.2)

Soil type	*T*	0.5s		0.8s		1.2s		2.0s	
	H	0.0566	0.2	0.0566	0.2	0.0566	0.2	0.0566	0.2
A	α	1.22	1.23	1.07	1.06	1.05	1.10	0.97	0.91
	β	1.08	1.08	0.99	1.05	1.10	1.05	0.92	1.02
B	α	1.19	1.14	1.07	1.04	1.05	0.99	1.04	1.02
	β	1.05	1.15	1.06	1.07	0.97	1.04	0.96	1.04
C	α	1.22	1.12	1.11	1.11	1.07	1.03	0.97	0.98
	β	1.08	1.09	1.16	1.19	1.06	1.06	0.99	1.10
D	α	1.14	1.14	1.06	1.05	0.95	1.03	0.92	0.92
	β	1.18	1.22	1.09	1.15	1.05	1.07	0.95	1.03

Table 2. The values of α and β identified from numerical results (*P*=0.53, 0.75 and 1.0)

Soil type	*T*	0.5s			0.8s			1.2s			2.0s		
	P	0.53	0.75	1.0	0.53	0.75	1.0	0.53	0.75	1.0	0.53	0.75	1.0
B	α	1.19	1.14	1.06	1.07	1.08	1.03	1.05	1.06	1.05	1.04	1.08	1.06
	β	1.05	1.10	1.15	1.06	1.05	1.04	0.97	0.99	0.91	0.96	0.91	0.86
D	α	1.14	1.10	1.01	1.06	1.03	1.01	0.95	0.97	1.03	0.92	0.97	1.01
	β	1.18	1.20	1.22	1.09	1.09	1.10	1.05	1.03	0.98	0.95	0.93	0.91

The coefficients of α and β for all cases are summarized in Table 1 and Table 2. These identified values suggest that the seismic sequences amplify the ductility demands in a certain level, depending on the intensity ratio. It is evident that the short period structure leads to a higher ratio of M_2/M_1. This behavior can be generalized for any soil type and any parameter of the pinching hysteretic models. However, for the bilinear model (*P*=1.0), a relatively smaller amplification effect is observed, and the influence of period can be ignored.

4.1.2 *Comparison of Displacements Induced by Repeated and Single Excitation*

In order to figure out the effect of the damage caused by the first ground motion, the ductility demand induced by the second ground motion in a seismic sequence is compared to the ductility demand induced by the same single ground motion. $M_{2,s}$ is used to denote the displacement of the later case. $M_2/M_{2,s}$ means the ratio of the ductility demand of a pre-damaged structure to the ductility demand of an intact structure. Figure 6 illustrates $M_2/M_{2,s}$ versus the intensity of the first ground motion in sequence, and the results are plotted by the intensity of the second ground motion. It is evident from Figure.6 that a pre-damaged structure experiences much larger displacement than an intact structure. This tendency becomes more prominent for short period structures. For the same PGA_1, a smaller PGA_2 leads to a larger ratio of $M_2/M_{2,s}$. Furthermore, when the pre-damage level is small, the ratio $M_2/M_{2,s}$ is also very small.

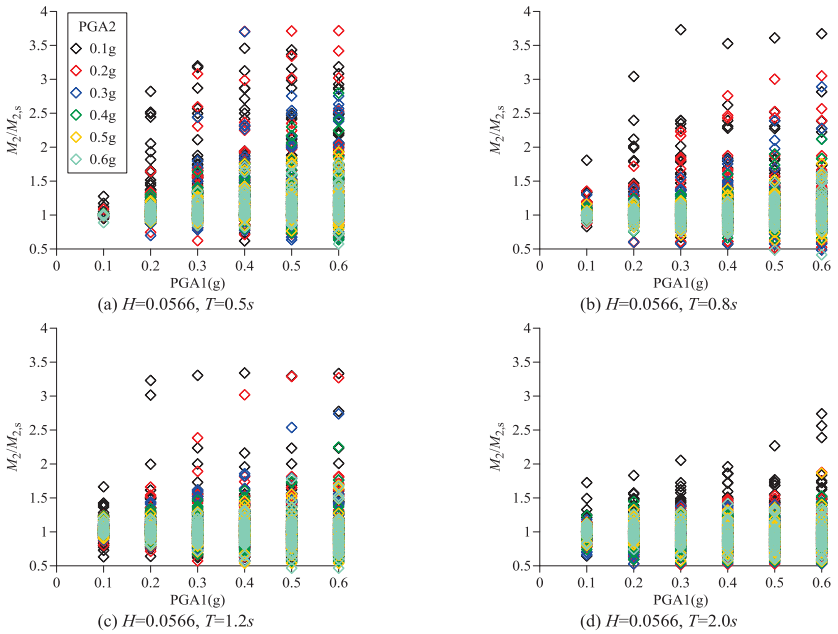

Figure 6. Ductility demand of pre-damaged buildings to ductility demand of intact building.

4.2 *Residual Displacement*

Residual displacement is an important index indicating the repairability of structure after the earthquake. The residual displacement is usually presented by the ratio of residudal displacement to the maximum displacement. The residual displacement of pinching hystretic strutures are statistically investigated, and only strutural models with H=0.0566 are considered. The residual displacement induced by the first and the second ground motion in a sequence are denoted by R_1 and R_2, respectively. Figure 7 displays the histograms for R_1/M_1 and R_2/M_2, accompanied with the kernel density estimation curve. The distributions of the ratio R_1/M_1 and R_2/M_2 are fitted by exponential distributions, which show relatively better accuracy than other distribution patterns. The probability distribution fucntions for R_1/M_1 and R_2/M_2 are given by Eq.(2) and Eq.(3), respectively.

$$\mathrm{PDF}\left(\frac{R_1}{M_1}\right) = 15.237e^{\left(-15.237\frac{R_1}{M_1}\right)} \tag{2}$$

$$\mathrm{PDF}\left(\frac{R_2}{M_2}\right) = 12.071e^{\left(-12.071\frac{R_2}{M_2}\right)} \tag{3}$$

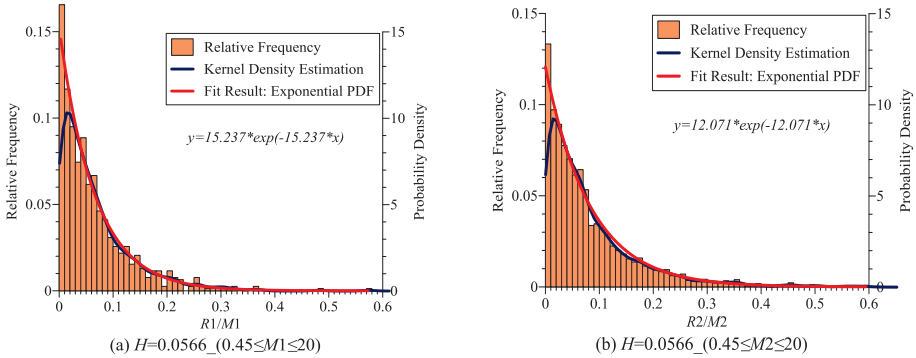

Figure 7. The probability density distribution of the residual displacement ratio.

The results suggest that the residual displacement R_1 has the probability of 79% of being smaller than 10% of the maximum displacement M_1, and this also means the same probability that structure experienced maximum displacement ten times the residual displacement. Compared to R_1, R_2 has a very similar distribution pattern, and the residual displacement ratio for R_2 is only a little larger than that for R_1 for a given probability level. The regressed probability density functions can be used to estimate the maximum displacement experienced by structure in a probabilistic way.

5 Conclusions

The responses of pinching hysteretic structures subjected to seismic sequences were investigated. The effect of seismic sequences on the ductility demand and residual displacement ratio were examined, and the conclusions are summarized as follows.

a) The seismic sequences lead to ductility demands higher than those derived from single seismic event. This effect is more significant for short-period structure subjected to ground motions of hard soil sites. Compared to bilinear hysteretic structures, seismic sequences have more significant effect on the pinching hysteretic structure. Therefore, it is essential to consider the sequence effect in seismic analyses to ensure the safety and integrity of the pinching hysteretic structure. Based on the numerical results, the ductility demand ratio is regressed as a function of intensity ratio of ground motions in a sequence.
b) The damage caused by the first seismic excitation affects the ductility level induced by a sequential excitation. This effect is influenced by the pre-damage level and the intensity of the second excitation in a sequence.
c) The residual displacement ratio of pinching hysteretic structure approximately obeys an exponential distribution. The fitted exponential distribution functions for residual displacement caused by the first and the second excitation in a sequence are very similar.

Acknowledgements

The research is supported by "The Fundamental Research Funds for the Central Universities (Grant No.185206006)".

References

Amadio, C., Fragiacomo, M., Rajgelj, S. The effects of repeated earthquake ground motions on the non-linear response of SDOF systems. *Earthq. Eng. Struct. D.* 32(2), 291-308, Feb, 2003.

Boore, D.M. Some notes concerning the determination of shear-wave velocity and attenuation. In: Proceedings of geophysical techniques for site and material characterization, 129-134, 1993.

Di Sarno, L., Yenidogan, C. and Erdik, M. Field evidence and numerical investigation of the Mw = 7.1 October 23 Van, Tabanli and the Mw > 5.7 November Earthquakes of 2011, *Bull Earthquake Eng*, 11(1), 313-346, Feb, 2013.

Hatzigeorgiou, G.D. and Beskos, D.E. Inelastic displacement ratios for SDOF structures subjected to repeated earthquakes. *Eng. Struct.* 31(11), 2744-2755, Nov, 2009.

Hatzigeorgiou, G.D. Ductility demand spectra for multiple near- and far-fault earthquakes. *Soil Dyn. Earthq. Eng*., 30(4), 170-183, Apr, 2010.

Kam, W.Y. and Pampanin, S. The Seismic Performance of RC Buildings in the 22 February 2011 Christchurch Earthquake, *Struct. Concrete*, 12(4), 223–233, Dec, 2011.

Matsuda, K. and Kasai, K. Passive Control Design Method for MDOF System Composed of Bilinear + Slip Model added with Visco-Elastic Damper. *J. Struct. Constr. Eng.*, 80(716), 1525-1535, 2015.

Shin, M. and Kim, B. Effects of frequency contents of aftershock ground motions on reinforced concrete (RC) bridge columns. *Soil Dyn. Earthq. Eng*. 97, 48-59, June, 2017.